雑誌

発表者氏名	論文タイトル名	発表誌名	巻号	ページ	出版年
Y. Miyamoto, T. Mukai, N. Nakata, Y. Maeda, M. Kai, T. Naka, I. Yano, M. Makino.	Identification and characterization of the genes involved in glycosylation pathways of mycobacterial glycopeptidolipids biosynthes is.	J. Bacteriol.	188(1)	86-95	2006
T. Mukai, Y. Miyamoto, T. Yamazaki, M. Makino.	Identification of *Mycobacterium* species by comp arative analysis of the *dnaA* gene.	FEMS Microbiol. Lettr.	254	232-239	2006
M. Makino, Y. Maeda, T. Mukai, S. H. E. Kaufmann.	Impaired maturation and function of dendritic cells by mycobacteria through IL-1β.	Eur. J. Immunol.	36	1443-1452	2006
K. Suzuki, N. Nakata, P. D. Bang, N. Ishii, M. Makino.	High-level expression of pseudogenes in *Mycobacterium leprae*.	FEMS Microbiol. Lettr.	259	208-214	2006
M. Makino, Y. Maeda, K. Inagaki.	Immunostimulatory activity of Recombinant *Mycobacterium bovis* BCG that secretes Major Membrane Protein II of *Mycobacterium leprae*.	Infect. Immunity	74(11)	6264-6271	2006
T. Kikuchi, S. Uehara, H. Ariga, T. Tokunaga, A. Kariyone, T. Tamura, K. Takatsu,	Augmented induction of $CD8^+$ cytotoxic T-cell response and antitumour resistanceby T hel pertype 1-induing peptide.	Immunology	117	47-58	2006
小林和夫	感染症の現状と制圧戦略.	都市問題研究	58	20-32	2006

Y. Ozeki, H. Tsutsui, N. Kawada, H. Suzuki, M. Kataoka, T. Kodama, I. Yano, K. Kaneda, K. Kobayashi.	Macrophage scavenger Receptor down-regulates mycobacterial cord factor-induced proinflammatory cytokine production by alveolar and hepatic macrophages.	Microb. Pathog.	40	171-176	2006
K. Suzuki, F. Takeshita, N. Nakata, N. Ishii, M. Makino.	Localization of CORO1A in the macrophages containing *Mycobacterium leprae*.	Acta Histochemica et Cytochemica	in press		2007
M. Makino, Y. Maeda, Y. Fukutomi, T. Mukai.	Contribution of GM-CSF on the enhancement of the T cell-stimulating activity of macrophages.	Microbes and Infection	in press		2007

第2章　病理・病態生理

結核の免疫

要旨

結核は，単一病原体による感染症としては人類に最も健康被害を及ぼしており，全世界で 20 億人（全人口の約 1／3）が結核菌に既感染，毎年 800 万人が結核を発病，200 万人が死亡し，有病者は 2,200 万人である[1]．結核菌の病原性の特徴として，① マクロファージに感染し宿主防御機構から逸脱する，② 潜伏感染により宿主からの排除を免れる，③ 遅延型過敏反応を誘導し組織破壊を伴う肉芽腫を形成する，といったことがある[2]．これらの特徴は，結核菌－宿主免疫応答との相互作用によって生じるものであり，結核の予防・治療戦略の構築には，結核に対する宿主免疫の理解が必須である．

●キーワード

結核菌－宿主関係
細胞性免疫
潜伏感染
サイトカイン
肉芽腫

はじめに

肺結核患者から喀痰排泄された結核菌の暴露者の約 30％ に結核菌感染が成立し，感染者の約 10％ が生涯中に結核を発症する．しかし，発症しない感染者も結核菌の体内からの完全な排除は不可能と考えられる．このことは，90％ の感染者は宿主防御機構によって結核菌の増殖を封じ込め発病を回避できるが，結核菌が宿主内で潜伏感染していることを意味する．潜伏感染した結核菌は，老化，免疫抑制療法［免疫抑制薬，ステロイド剤，抗サイトカイン療法：腫瘍壊死因子 α（TNFα）阻害薬など］，栄養障害，ヒト免疫不全ウイルス（HIV）感染／後天性免疫不全症候群（AIDS）などの宿主免疫機構の低下により，発育，増殖を再開し，結核を発症するに至る．これを内因性再燃と呼ぶ．一般的に成人では，潜伏感染の内因性再燃の形で結核を発症することが多い．一方，小児や HIV 感染／AIDS 患者では，初感染によって結核を発症しうる．

結核発症を規定する遺伝的因子として，ヒト第 2 染色体に存在する遺伝子 solute carrier family 11 member 1（SLC11a1）／natural re-

sistance associated macrophage protein 1（Nramp1）が同定された．この遺伝子はマクロファージに発現しており，食胞内から細胞質への鉄イオンの輸送タンパクを規定する．鉄イオンは結核菌の食胞内増殖に必須な物質であり，宿主－結核菌間の鉄の競合により，感染抵抗性を発揮すると考えられる[3]．

結核菌の既感染の有無は，遅延型過敏反応（DTH）であるツベルクリン反応や結核菌特異的抗原による末梢血単核細胞インターフェロンγ（IFNγ）遊離試験（QuantiFERON－2G®など）によって判定されるが，ツベルクリンに対する免疫応答は結核再燃における生体防御に必ずしも役立っていないと考えられる．事実，現行ワクチンであるBCG は一次結核の発症予防に極めて有効であるが，潜伏感染からの再燃である成人の結核にはほとんど無効である．すなわち，初感染やBCG 接種によって誘導される初感染に有効な免疫応答は，再燃を阻止する免疫応答と異なることが考えられる[4]．

結核菌初期感染における防御免疫

結核菌感染は主として生菌を含む飛沫核の吸入によって成立する．気道を介し侵入した結核菌は，肺胞マクロファージによって貪食される．一般的な細菌はマクロファージ食胞内で殺菌されるのに対し，結核菌はマクロファージ食胞体（ファゴソーム）と多量の加水分解酵素を含む水解小体（リソソーム）の融合を阻害することにより，食胞内pH の低下を伴う食胞の成熟を防ぎ，食胞内で生存し続ける細胞内寄生細菌である（表1）．

静止期にあるマクロファージは細胞内結核菌の殺菌を行うことはできないが，IFNγ などの物質で活性化されると食胞が成熟して菌を融解するとともに，反応性酸素化合物（ROI）や反応性窒素化合物（RNI）産生を誘導し，結核菌を殺菌することができるようになる．したがって，結核菌感染防御にかかわっている宿主防御因子は，自然免疫だけではなく，マクロファージ，サイトカイン，CD4 陽性1型ヘルパーT（Th1）細胞の協調が必要である．加えて，CD8 陽性キラーT細胞（CTL）による感染マクロファージ傷害や細菌の直接障害も重要な宿主防御因子であると考えられている．γδT 細胞や CD1 拘束性T細胞は，脂質抗原など非タンパク性抗原を認識する免疫機構

表1　結核菌の特徴

細胞内寄生性	桿菌（0.2～0.6×1～10 μm），宿主細胞，特にマクロファージ内で抗菌機構から逃れて増殖
細胞壁	脂質成分が豊富なため疎水性であり，化学物質にも安定，グラム染色に難染色性，抗酸性
好気性	酸素分圧の高い臓器（肺など）で増殖し，病変を形成
遅発育性	至適温度：37 ℃，倍加時間：約 12～15 時間，培養集落形成に 4～8 週間
感染形式	飛沫核/空気感染
病原性	慢性炎症，肉芽腫，乾酪壊死，空洞形成，線維化
遺伝子	全ゲノム（約 4.41 Mb）の解読

として近年注目されている[5]．一部のT細胞はメモリーT細胞へと分化し，再燃の際に速やかに効率よく免疫応答を誘導し，再発を防ぐように働くと考えられる．

感染マクロファージや結核菌抗原を補足した樹状細胞は肺門リンパ節などの所属リンパ節へ走化し，リンパ節において感染マクロファージあるいは樹状細胞は細胞表面の主要組織適合性抗原複合体（MHC）に結核菌抗原を提示する．その後，結核特異的T細胞を誘導し，初期獲得免疫応答が成立する[6]．結核菌成分を Toll 様受容体（TLR）などによって認識することで，活性化された抗原提示細胞は Th1 指向性サイトカイン：インターロイキン（IL）－12 や IL－18 を産生し，抗原特異的 CD4 陽性T細胞を典型的な Th1 細胞へ分化させ，これらの細胞が大量の IFNγ，TNFα やリンホトキシンα（LTα）などの Th1 サイトカインを産生する（図1）[7]．分化したT細胞は感染局所へ移動し，結核特異的免疫応答を増強させる．しかし，Th1 細胞－サイトカイン－マクロファージ相互作用でマクロファージが活性化されても完全な菌の排除は達成できず，一部のマクロファージ内結核菌は増殖を停止し，代謝も低下させて休眠状態となり，潜伏感染へと移行する．

図1　微生物感染における細胞性および液性免疫応答

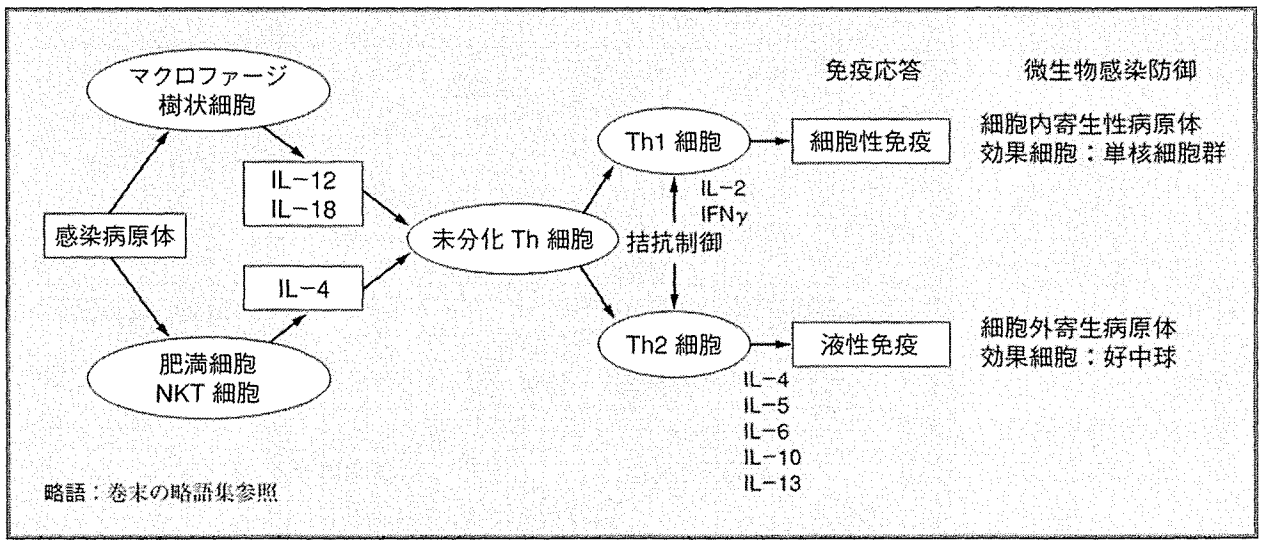

結核性肉芽腫炎症と免疫応答

結核病変の特徴である肉芽腫病変の本態は，排除不能な異物もしくは病原体を局所に封じ込め，あるいは宿主組織に害を及ぼすことなく，高濃度の効果機能分子を作用させるために誘導される限局性慢性炎症である．肉芽腫は，発症機序により，T細胞免疫応答非依存性異物性肉芽腫と依存性過敏性肉芽腫に分類される．初期感染において殺菌できない結核菌を封じ込めるため，マクロファージは TNFα や IL−1 などの炎症性サイトカイン産生と，それらのサイトカインによって誘導される単球走化性タンパク質（MCP−1；CCL2）やマクロファージ炎症性タンパク（MIP−1；CCL3，CCL4）を介して，病巣への単球/マクロファージの流入・集積を促し，異物性肉芽腫を形成する[8~11]．他方，獲得免疫応答の結果産生される IFNγ は肉芽腫病変内マクロファージから IFNγ 誘導性モノカイン（MIG；CXCL9）や IFNγ 誘導性タンパク−10（IP−10；CXCL10），IFNγ 誘導性T細胞遊走因子α（I−TAC；CXCL11）などの産生を介して，Th1 細胞の肉芽腫内集積を惹起し，過敏性肉芽腫反応を誘導する[12]．したがって，結核性肉芽腫病変は成因論的に両者が複合した混合性肉芽腫病変である（図2）．

結核性肉芽腫形成における菌側因子として，抗酸菌細胞壁に存在する糖脂質が注目されている．特にアシル化トレハロース脂質化合物である trehalose 6, 6′−dimycolate（TDM）/ code factor やスルホリピ

図2　結核性肉芽腫炎症の細胞・機能分子機序

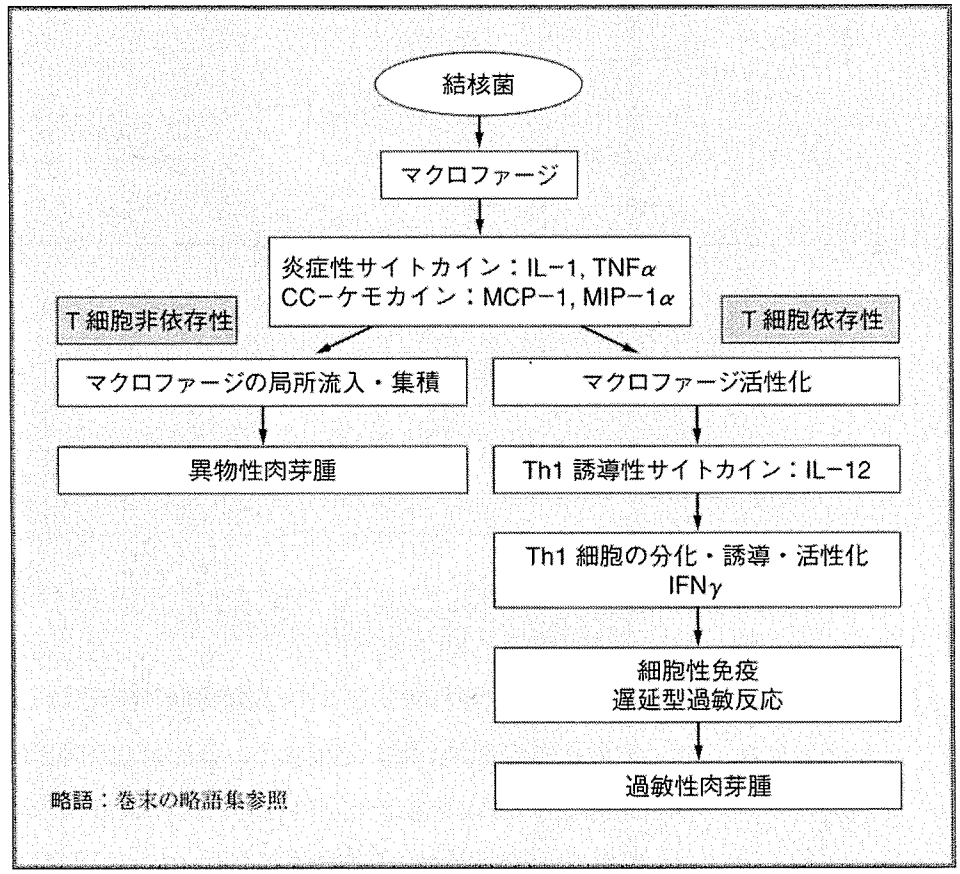

ド（SL）が宿主防御機能を修飾し，結核菌の病原性に関与している．TDM と SL は貪食マクロファージ内でリソソームと結核菌を含む食胞の融合を阻害する．さらに，TDM は結核と同じ混合性肉芽腫性炎症を誘導する[10]．また，肉芽腫形成に病変局所における末梢血細胞の流入，すなわち血管因子が必須であるが，TDM は血管内皮細胞増殖因子（VEGF）を誘導し，血管新生にも寄与している[13]．加えて，TDM はリンパ組織の宿主免疫担当細胞にアポトーシスを誘導し，自己反応性T細胞の除去，Th1 / Th2 細胞の分化を抑制することにより自己免疫疾患の発症を抑制している可能性がある（図3）[14]．すなわち，TDM は結核菌－宿主関係における多機能分子である．

通常の初期感染において肉芽腫に封じ込められた結核菌は，増殖に必要である酸素分圧の低下によって休眠を余儀なくされる．この病変は小型で，咳嗽や喀痰など臨床症状を伴わず，胸部X線検査でわずかに認められる初期病巣として知られている．

免疫能低下などで結核菌が休眠から再活性化すると，内因性再燃に

図3　結核菌細胞壁 TDM と宿主応答の分子機序

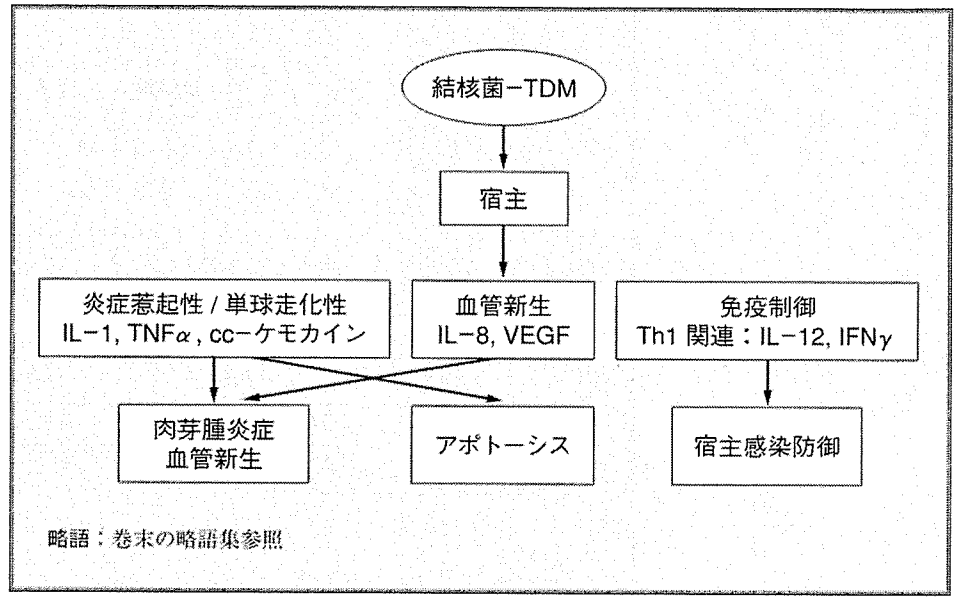

よる二次結核を発症する．この型の結核性肉芽腫の特徴として，肉芽腫の中心に乾酪壊死が出現し，外部と交通して空洞ができる．乾酪壊死による豊富な脂質と高濃度の酸素は結核菌の増殖に適しており，臨床的な結核を発症するに至る．しかし，AIDS 患者[15]やT細胞欠損動物[16]などT細胞性免疫に欠陥がある場合，乾酪壊死や空洞形成が認められないことから，T細胞免疫が結核の病態に負の役割を演じていることが推察される．したがって，結核菌に対する遅延型過敏反応を含む細胞性免疫応答は，抗結核防御と組織障害，すなわち功罪の二面性を持つ諸刃の剣であると考えられる[17]．以上のことから，宿主生体防御と結核菌増殖のバランスによって，結核の病態が形成されることが分かる（図4）．この平衡状態が生涯続く場合には結核を発症しない．しかし，潜伏感染における免疫応答，あるいは再燃の防御に働く免疫応答については十分に明らかになっていない．

結核の再燃を阻止する免疫応答が，初期感染に有効な免疫応答と異なる理由として，抗酸菌が増殖期と休眠期に発現する遺伝子を著しく変化させる可能性が挙げられる．遅延発育型抗酸菌が定常期や休眠期において最も大量に発現するタンパク質である mycobacterial DNA−binding protein−1（MDP1）は，抗酸菌体内や表層に存在する抗酸菌特異的タンパク質である．機能的に細胞内 MDP1 は核酸結合性を有し，転写および翻訳阻害活性を持ち，そのため休眠機構，さらに潜

図4　抗酸菌 / 結核菌感染における宿主細胞および機能分子応答機構

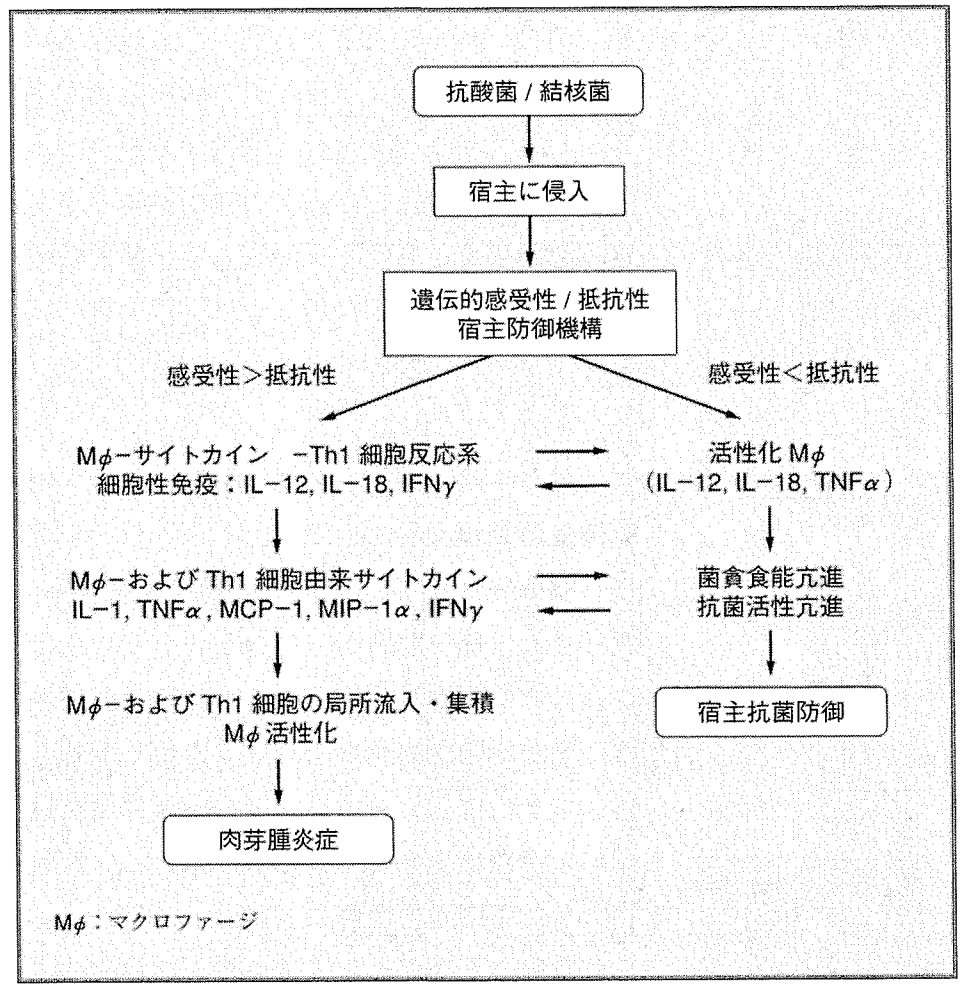

伏感染に関与していることが示唆されている．他方，菌表層 MDP1 が宿主細胞表面に存在するムコ多糖（グルコサアミノグルカン），特にヒアルロン酸に結合し，MDP1 が抗酸菌の宿主細胞への接着 / 侵入に関与する接着分子であることが判明[18] し，加えて，宿主が MDP1 に対し Th1 細胞応答など防御免疫を発現すること[19] が判明し，今後の治療・予防標的候補として期待される．

おわりに

結核菌感染において，結核菌の Th1 誘導能によって，細胞性免疫応答が成立し発症を阻止する．しかし，結核菌が潜伏感染し，細胞性免疫の負の側面である DTH による肉芽腫が必ずしも宿主に有利に働かないため，結核の増殖は抑制できるが，感染宿主における結核菌の完全排除はできず，免疫能が低下すると結核を発症する．初期感染と

再燃結核の防御に必要な免疫応答は異なることが予想され，現在の結核対策上，極めて重要な課題である成人肺結核に対するワクチンや治療戦略の開発には，休眠状態の結核菌で特異的に発現する分子の探索，さらに成人結核の大部分を構成する内因性再燃や外来性再感染による二次結核に有効な免疫応答の解明が必要であろう．結核菌－宿主防御免疫の関係をより良く理解することが，結核の制圧戦略を構築するうえで必須である．

謝　辞

筆者らの研究は厚生労働省厚生労働科学研究費補助金（新興・再興感染症研究事業），文部科学省科学研究費補助金（特定領域研究および基盤研究C），日米医学協力研究会結核・ハンセン病専門部会，大阪市立大学都市問題研究費および大阪結核研究会により支援された．

阿戸　学・小林和夫

文　献

1) Hingley-Wilson SM, et al: Survival perspectives from the world's most successful pathogen, Mycobacterium tuberculosis. Nat Immunol 4 (10): 949–955, 2003.
2) Smith I: Mycobacterium tuberculosis pathogenesis and molecular determinants of virulence. Clin Microbiol Rev 16 (3): 463–496, 2003.
3) Hackam DJ, et al: Host resistance to intracellular infection: mutation of natural resistance-associated macrophage protein 1 (Nramp1) impairs phagosomal acidification. J Exp Med 188 (2): 351–364, 1998.
4) Kaufmann SH: Is the development of a new tuberculosis vaccine possible? Nat Med 6 (9): 955–960, 2000.
5) Brigl M, et al: CD1: antigen presentation and T cell function. Annu Rev Immunol 22: 817–890, 2004.
6) Kaufmann SH: Recent findings in immunology give tuberculosis vaccines a new boost. Trends Immunol 26 (12): 660–667, 2005.
7) North RJ, et al: Immunity to tuberculosis. Annu Rev Immunol 22: 599–623, 2004.
8) Kobayashi K, et al: Strain variation of bacillus Calmette-Guerin-induced pulmonary granuloma formation is correlated with anergy and the local production of migration inhibition factor and interleukin 1. Am J Pathol 119 (2): 223–235, 1985.
9) Sato IY, et al: Regulation of Mycobacterium bovis BCG and foreign body granulomas in mice by the Bcg gene. Infect Immun 58 (5): 1210–1216, 1990.
10) Yamagami H, et al: Trehalose 6, 6'-dimycolate (cord factor) of Mycobacterium tuberculosis induces foreign-body-and hyper-

sensitivity-type granulomas in mice. Infect Immun 69 (2): 810-815, 2001.
11) Kasahara K, et al: Selective expression of monocyte chemotactic and activating factor/monocyte chemoattractant protein 1 in human blood monocytes by Mycobacterium tuberculosis. J Infect Dis 170 (5): 1238-1247, 1994.
12) Fuller C L, et al: In situ study of abundant expression of proinflammatory chemokines and cytokines in pulmonary granulomas that develop in cynomolgus macaques experimentally infected with Mycobacterium tuberculosis. Infect Immun 71 (12): 7023-7034, 2003.
13) Saita N, et al: Trehalose 6, 6'-dimycolate (cord factor) of Mycobacterium tuberculosis induces corneal angiogenesis in rats. Infect Immun 68 (10): 5991-5997, 2000.
14) Hamasaki N, et al: In vivo administration of mycobacterial cord factor (Trehalose 6, 6'-dimycolate) can induce lung and liver granulomas and thymic atrophy in rabbits. Infect Immun 68 (6): 3704-3709, 2000.
15) Long R, et al: The chest roentgenogram in pulmonary tuberculosis patients seropositive for human immunodeficiency virus type 1. Chest 99 (1): 123-127, 1991.
16) Ehlers S, et al: Alphabeta T cell receptor-positive cells and interferon-gamma, but not inducible nitric oxide synthase, are critical for granuloma necrosis in a mouse model of mycobacteria-induced pulmonary immunopathology. J Exp Med 194 (12): 1847-1859, 2001.
17) Kobayashi K, et al: Immunopathogenesis of delayed-type hypersensitivity. Microsc Res Tech 53 (4): 241-245, 2001.
18) Aoki K, et al: Extracellular mycobacterial DNA-binding protein 1 participates in mycobacterium-lung epithelial cell interaction through hyaluronic acid. J Biol Chem 279 (38): 39798-39806, 2004.
19) Matsumoto S, et al: DNA augments antigenicity of mycobacterial DNA-binding protein 1 and confers protection against *Mycobacterium tuberculosis* infection in mice. J Immunol 175 (1): 441-449, 2005.

JOURNAL OF BACTERIOLOGY, Jan. 2006, p. 86–95 Vol. 188, No. 1
0021-9193/06/$08.00+0 doi:10.1128/JB.188.1.86–95.2006

Identification and Characterization of the Genes Involved in Glycosylation Pathways of Mycobacterial Glycopeptidolipid Biosynthesis

Yuji Miyamoto,[1] Tetsu Mukai,[1] Noboru Nakata,[1] Yumi Maeda,[1] Masanori Kai,[1] Takashi Naka,[2] Ikuya Yano,[2] and Masahiko Makino[1]*

Department of Microbiology, Leprosy Research Center, National Institute of Infectious Diseases, 4-2-1 Aobacho, Higashimurayama, Tokyo 189-0002, Japan,[1] and Japan BCG Central Laboratory, 3-1-5 Matsuyama, Kiyose, Tokyo 204-0022, Japan[2]

Received 2 August 2005/Accepted 10 October 2005

Glycopeptidolipids (GPLs) are major components present on the outer layers of the cell walls of several nontuberculous mycobacteria. GPLs are antigenic molecules and have variant oligosaccharides in mycobacteria such as *Mycobacterium avium*. In this study, we identified four genes (*gtf1*, *gtf2*, *gtf3*, and *gtf4*) in the genome of *Mycobacterium smegmatis*. These genes were independently inactivated by homologous recombination in *M. smegmatis*, and the structures of GPLs from each gene disruptant were analyzed. Thin-layer chromatography, gas chromatography–mass spectrometry, and matrix-assisted laser desorption ionization–time-of-flight mass spectrometry analyses revealed that the mutants Δgtf1 and Δgtf2 accumulated the fatty acyl-tetrapeptide core having *O*-methyl-rhamnose and 6-deoxy-talose as sugar residues, respectively. The mutant Δgtf4 possessed the same GPLs as the wild type, whereas the mutant Δgtf3 lacked two minor GPLs, consisting of 3-*O*-methyl-rhamnose attached to *O*-methyl-rhamnose of the fatty acyl-tetrapeptide core. These results indicate that the *gtf1* and *gtf2* genes are responsible for the early glycosylation steps of GPL biosynthesis and the *gtf3* gene is involved in transferring a rhamnose residue not to 6-deoxy-talose but to an *O*-methyl-rhamnose residue. Moreover, a complementation experiment showed that *M. avium gtfA* and *gtfB*, which are deduced glycosyltransferase genes of GPL biosynthesis, restore complete GPL production in the mutants Δgtf1 and Δgtf2, respectively. Our findings propose that both *M. smegmatis* and *M. avium* have the common glycosylation pathway in the early steps of GPL biosynthesis but differ at the later stages.

The mycobacterial cell envelope has a unique structure that contains a complex of covalently linked peptidoglycan, arabinogalactan, and mycolic acids (7, 11). The outer layer of the cell envelope is composed of several types of glycolipids that affect the surface properties of mycobacterial cells (7, 11). Glycopeptidolipids (GPLs) are a major class of glycolipid present on the outer layer of several species of nontuberculous mycobacteria, such as *Mycobacterium avium* complex, *M. scrofulaceum*, *M. chelonae*, *M. fortuitum*, and *M. smegmatis* (31). GPLs have a common fatty acyl-tetrapeptide core consisting of tetrapeptide amino alcohol (D-Phe-D-*allo*-Thr-D-Ala-L-alaninol) and amide-linked long-chain fatty acid (C_{26-34}). The fatty acyl-tetrapeptide core is glycosylated with 6-deoxy-talose (6-d-Tal) and variable *O*-methyl-rhamnose (*O*-Me-Rha) residues, termed non-serovar-specific GPLs (nsGPLs), which are also the main products of *M. smegmatis* GPLs (1, 4, 10). The GPLs of *M. avium* have a more complicated structure, in which an additional Rha residue is added to 6-d-Tal of nsGPLs to be extended with various haptenic oligosaccharides, which are important surface antigens, resulting in serovar-specific GPLs (ssGPLs) (1, 4, 31).

There are some evidences that GPLs may be responsible for pathogenicity. It has been shown that the some of the ssGPLs are immunosuppressive and are able to induce a variety of cytokines, which affect host responses to infection (3, 15, 18, 29). Also, ssGPLs are identified as the factors modulating the phagocytosis and phagosome-lysosome fusion (17, 21). The altered GPL structure is also known to affect the colony morphology relevant to variable virulence (14, 30).

The biosyntheses of GPLs, particularly nsGPLs, have been characterized for *M. smegmatis*. Several biosynthetic genes encoding enzymes such as *O*-methyltransferase, acetyltransferase, and peptide synthetase have been identified (5, 16, 25, 26), but less is known about the genes involved in the glycosylation steps of the GPLs. The only glycosyltransferase gene that has been characterized is *rtfA* from *M. avium*, which is responsible for transferring the Rha residue to 6-d-Tal of nsGPLs to form ssGPLs (12). However, the initial glycosylation steps for the formation of nsGPLs remain unknown. Recently, it was shown that GPLs from *M. smegmatis* has a unique structure in which nsGPLs are further glycosylated, unlike ssGPLs (23, 24, 32), but these unique GPLs are produced in a carbon-starved situation, which is not a normal growth condition.

In this study, to clarify the glycosylation step leading to the formation of nsGPLs and its further products, we focused on four of the *M. smegmatis* genes having high similarity to *M. avium rtfA*, whose functions remain uncharacterized. Here, we have undertaken the gene disruption approach for generating each mutant in *M. smegmatis*, characterized their biochemical phenotypes, and finally hypothesized new biosynthetic pathways associated with glycosylation of GPLs.

* Corresponding author. Mailing address: Department of Microbiology, Leprosy Research Center, National Institute of Infectious Diseases, 4-2-1 Aobacho, Higashimurayama, Tokyo 189-0002, Japan. Phone: 81-42-391-8059. Fax: 81-42-391-8212. E-mail: mmaki@nih.go.jp.

TABLE 1. Bacterial strains and vectors used in this study

Strain or vector	Characteristic(s)	Source or reference
Bacteria		
E. coli		
DH5α	Cloning host	
STBL2	Cloning host	
M. smegmatis		
mc^2155	Wild type	27
Δgtf1	*gtf1* disruptant	This study
Δgtf2	*gtf2* disruptant	This study
Δgtf3	*gtf3* disruptant	This study
Δgtf4	*gtf4* disruptant	This study
M. avium		
JATA51-01 (ATCC 25291)	Source of *gtfA* and *gtfB*	
Vectors		
pYUB854	Cosmid vector	2
phAE87	Phasmid vector carrying full-length DNA of mycobacteriophage PH101	2
pMV261	*E. coli-Mycobacterium* shuttle vector carrying *hsp60* promoter cassette	28
pYUBgtf1	pYUB854 with *gtf1*-disrupted sequences for generating recombinant mycobacteriophage	This study
pYUBgtf2	pYUB854 with *gtf2*-disrupted sequences for generating recombinant mycobacteriophage	This study
pYUBgtf3	pYUB854 with *gtf3*-disrupted sequences for generating recombinant mycobacteriophage	This study
pYUBgtf4	pYUB854 with *gtf4*-disrupted sequences for generating recombinant mycobacteriophage	This study
pMVgtf1	pMV261 with *gtf1*	This study
pMVgtf2	pMV261 with *gtf2*	This study
pMVgtf3	pMV261 with *gtf3*	This study
pMVgtf4	pMV261 with *gtf4*	This study
pMVgtfA	pMV261 with *gtfA*	This study
pMVgtfB	pMV261 with *gtfB*	This study

MATERIALS AND METHODS

Bacterial strains, culture conditions, and DNA manipulation. Bacterial strains and vectors used and constructed are listed in Table 1. Mycobacterial strains for DNA manipulation were grown in Middlebrook 7H9 broth (Difco) with 0.05% Tween 80 or Middlebrook 7H10 agar (Difco) with 0.5% glycerol, and each was supplemented with 10% albumin-dextrose-catalase enrichment (Difco). *M. smegmatis* strains for GPL production were cultured in Luria-Bertani (LB) broth with 0.05% Tween 80. DNA manipulation including isolation of DNA, transformation, and PCR was carried out as described previously (22). *E. coli* strain DH5α was used for routine manipulation and propagation of plasmid DNA. *E. coli* strain STBL2 was used for construction of phasmid vectors derived from phAE87. Antibiotics was added as required: kanamycin, 50 μg/ml for *E. coli* and 25 μg/ml for *M. smegmatis*; hygromycin B, 150 μg/ml for *E. coli* and 75 μg/ml for *M. smegmatis*.

Generation of the gene disruptants. The targeted genes (*gtf1*, *gtf2*, *gtf3*, and *gtf4*) were selected by BLAST analysis of unfinished *M. smegmatis* genome sequences deposited in the database of The Institute for Genomic Research (TIGR) (http://www.tigr.org) with the *rtfA* gene of *M. avium* as the query nucleotide sequence. Each gene was inactivated by inserting a hygromycin-resistant cassette (*hyg*) using the specialized transducing phage system (2). To construct the disrupted sequences, around 1.0-kb fragments both upstream and downstream of each gene were amplified from *M. smegmatis* mc^2155 genomic DNA using the following two pairs of primers: US1 and UA1 for upstream of *gtf1* and DS1 and DA1 for downstream of *gtf1*; US2 and UA2 for upstream of *gtf2* and DS2 and DA2 for downstream of *gtf2*; US3 and UA3 for upstream of *gtf3* and DS3 and DA3 for downstream of *gtf3*; US4 and UA4 for upstream of *gtf4* and DS4 and DA4 for downstream of *gtf4*. The PCR products were digested with each restriction enzyme and cloned into the corresponding sites flanking *hyg* of pYUB854 to give pYUBgtf1 (*gtf1*), pYUBgtf1 (*gtf2*), pYUBgtf3 (*gtf3*), and pYUBgtf4 (*gtf4*). These plasmids were used for packaging into the phasmid vector phAE87 to construct a specialized transducing mycobacteriophage for gene disruption as described previously (2). The *M. smegmatis* mc^2155 strain infected with the above mycobacteriophage at a multiplicity of infection of 10 was incubated at 37°C for 3 h in 7H9 broth without Tween 80. Harvested bacterial cells were then plated and cultured on 7H10 agar containing 75 μg/ml hygromycin B for 1 week. The hygromycin B-resistant colonies were selected, and their genomic DNA was subjected to PCR analysis to confirm the disruption of each gene using the following primers: U1 and D1 for *gtf1*; U2 and D2 for *gtf2*; U3 and D3 for *gtf3*; and U4 and D4 for *gtf4* (Fig. 1A to D).

Construction of the *gtf* expression vectors. The *gtf* genes of *M. smegmatis* and *M. avium* were amplified from each genomic DNA using the following primers: GTF1S and GTF1A for *gtf1*, GTF2S and GTF2A for *gtf2*, GTF3S and GTF3A for *gtf3*, GTF4S and GTF4A for *gtf4*, GTFAS and GTFAA for *gtfA*, and GTFBS and GTFBA for *gtfB*. The PCR products were digested with each restriction enzyme and cloned into the corresponding site of pMV261 to give pMVgtf1 (for the *gtf1* gene), pMVgtf2 (for the *gtf2* gene), pMVgtf3 (for the *gtf3* gene), pMVgtf4 (for the *gtf4* gene), pMVgtfA (for the *gtfA* gene), and pMVgtfB (for the *gtfB* gene). These vectors were used for complementation and overexpression experiment.

Isolation and purification of GPLs. The total lipids were extracted from harvested bacterial cells with $CHCl_3/CH_3OH$ (2:1, vol/vol) for several hours at room temperature. The extracts from the organic phase were separated from the aqueous phase and evaporated to dryness. For isolation of crude deacylated GPLs, total lipid fractions were subjected to mild alkaline hydrolysis as previously described (22, 25). For analytical thin-layer chromatography (TLC), the total lipid fraction after mild alkaline hydrolysis was spotted on silica gel 60 plates (Merck) and developed in $CHCl_3$-CH_3OH (9:1 [vol/vol]). Deacylated GPLs and other compounds were visualized by spraying with 10% H_2SO_4 and charring. Each total lipid fraction was extracted from an equal weight of harvested cells. Purified deacylated GPLs were separated from the total lipid fraction after mild alkaline hydrolysis by preparative TLC on the same plates and extracted from the bands corresponding to each GPLs. β-Elimination and perdeuteriomethylation treatment for determination of the linkage positions of sugar moieties were carried out as described previously (6, 9, 12).

GC/MS analysis. For monosaccharide analysis, purified deacylated GPLs or total lipid fraction after mild alkaline hydrolysis was hydrolyzed in 2 M trifluoroacetic acid (2 h, 120°C), and released sugars from deacylated GPLs were reduced with $NaBD_4$ (sodium borodeuteride) and then acetylated with pyridine-acetic anhydride (1:1 [vol/vol]) at room temperature overnight. Each total lipid fraction was extracted from an equal weight of harvested cells. The resulting

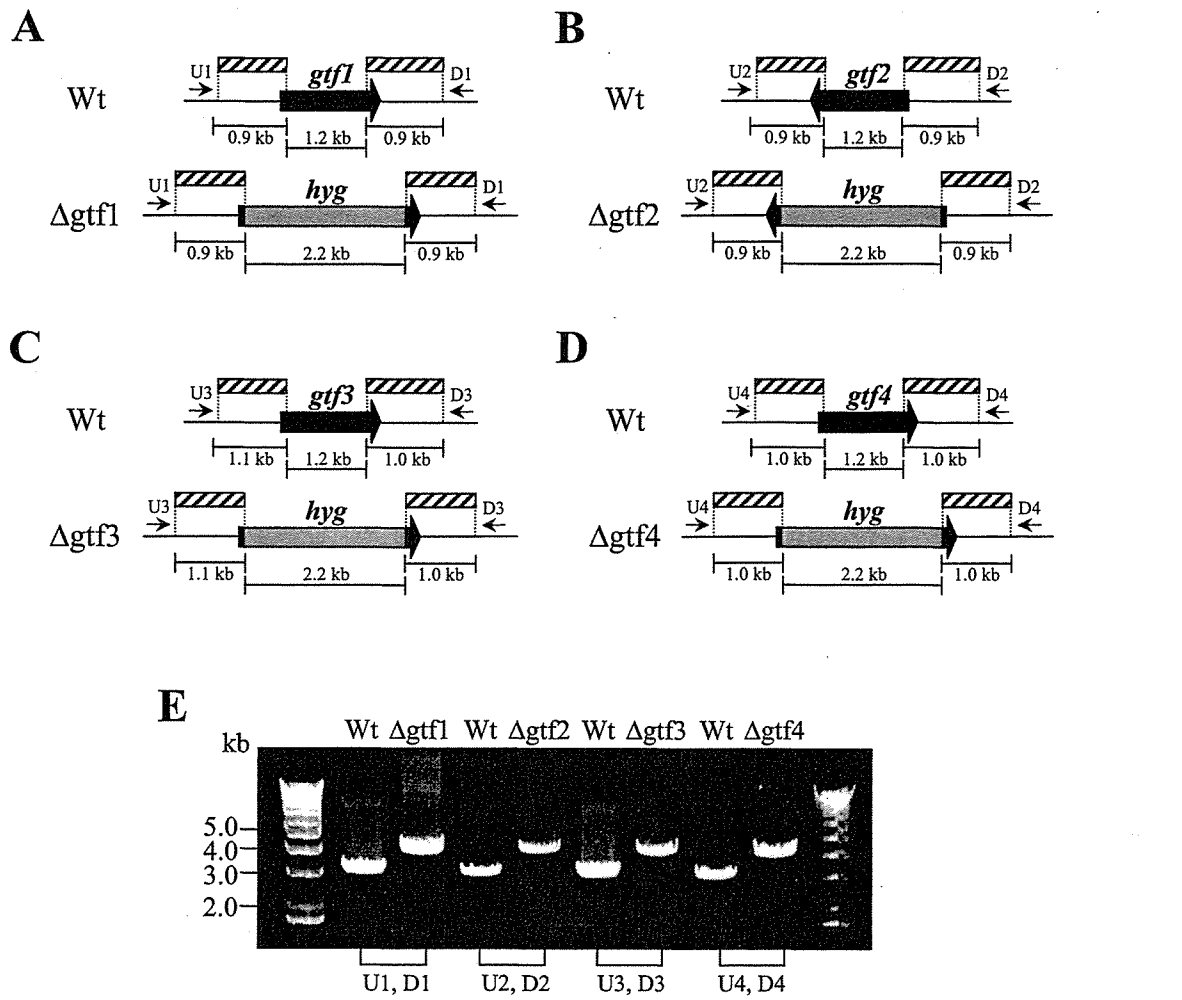

FIG. 1. Generation of *gtf* gene disruptants. (A to D) Schematic diagram of each *gtf* region on the chromosome of the wild-type *M. smegmatis* mc^{2}155 strain (Wt) and its gene disruptants Δgtf1, Δgtf2, Δgtf3, and Δgtf4. The shaded boxes indicate the regions included in recombinant phage for gene disruption. The black arrows represent the coding region of each *gtf* gene. The gray boxes represent the hygromycin resistance cassette (*hyg*). The primers used for PCR analysis are indicated by small arrows. (E) PCR analyses of the wild type and each disruptant using the primers indicated above.

alditol acetates were separated and analyzed by gas chromatography–mass spectrometry (GC/MS) on TRACE DSQ (Thermo electron) instrument equipped with an SP-2380 column (SUPELCO) using helium gas. The temperature program was from 52 to 172°C at 40°C/min and then 172 to 250°C at 3°C/min.

MALDI-TOF/MS analysis. To determine the total mass of the purified deacylated GPLs, matrix-assisted laser desorption ionization–time-of-flight (MALDI-TOF) mass spectra (in the positive mode) were acquired on a QSTAR XL (Applied Biosystems) with a pulse laser emitting at 337 nm. Samples mixed with 2,5-dihydroxybenzoic acid as the matrix were analyzed in the reflectron mode with an accelerating voltage operating in positive ion mode of 20 kV.

RESULTS

Disruption of *gtf1*, *gtf2*, *gtf3*, and *gtf4* by allelic exchange. Four genes showing high similarity to the *rtfA* gene, involved in GPL biosynthesis of *M. avium*, were identified for the *M. smegmatis* mc^{2}155 strain (12). The homologies of their corresponding amino acid sequences with that of RtfA were around 60%. Three genes were found in the GPL biosynthetic gene cluster, namely, *gtf1*, *gtf2*, and *gtf3* (GenBank accession no. AY138899.1) (16), whereas one gene, designated *gtf4* (TIGR database no. 4839918 to 4841162), was located far from the other three genes. To examine whether these genes are responsible for GPL biosynthesis, we generated four gene disruptants, designated Δgtf1, Δgtf2, Δgtf3, and Δgtf4, using the specialized transducing mycobacteriophage containing the entire open reading frame, replacing with the hygromycin resistance cassette (2). For confirmation of the gene disruption, PCR analysis was performed on chromosomal DNA from each disruptant. To avoid the amplification of disrupted sequences derived from residual mycobacteriophage, we designed and used the primers located outside the sequences included in each mycobacteriophage as shown in Fig. 1A to D. As expected, around 3.0-kb fragments were amplified from mc^{2}155 (wild type), whereas around 4.0-kb fragments were amplified from each disruptant, because most of the *gtf* coding region (1.2 kb) was replaced by the hygromycin resistance cassette (2.2 kb) (Fig. 1E). These results demonstrated that allelic exchanges involving replacement of the *gtf* genes with the disrupted constructs have been successful.

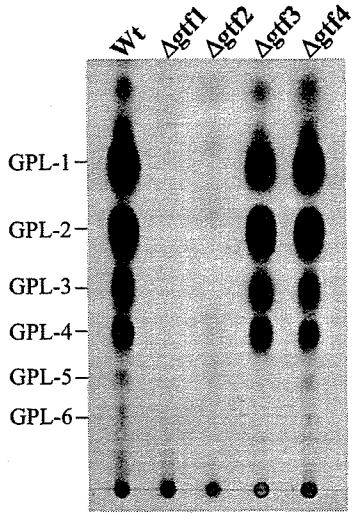

FIG. 2. TLC analyses of crude GPL extracts from the *M. smegmatis* mc^2155 strain (Wt) and its gene disruptants. The total lipid fraction after mild alkaline hydrolysis was spotted on plates and developed in $CHCl_3$-CH_3OH (9:1 [vol/vol]). GPLs were visualized by spraying with 10% H_2SO_4 and charring. Each total lipid fraction was extracted from an equal weight of harvested cells.

TLC analysis of gene disruptants. To investigate the effects of the mutation in each *gtf* gene, we examined GPL production of four gene disruptants. TLC analyses of total lipid fraction after mild alkaline hydrolysis revealed that wild-type mc^2155 mainly produced six components, designated GPL-1 to -6, whereas Δgtf1 and Δgtf2 lacked all six components and Δgtf3 lacked two minor ones (GPL-5 and GPL-6) found in the wild type (Fig. 2). In contrast, no differences in TLC profile were observed between Δgtf4 and the wild type (Fig. 2).

Characterization of Δgtf1 and Δgtf2. In Δgtf1 and Δgtf2, the TLC analyses showed that six GPL components contained in the wild type had disappeared. On the other hand, there is the possibility that both disruptants contained GPL derivatives which are structurally incomplete and hard to be detected by TLC analyses. To characterize the sugars included in GPL derivatives from both disruptants and to compare with the wild type, each total lipid fraction after mild alkaline hydrolysis was hydrolyzed, and the released monosaccharides as their alditol acetates were examined by GC/MS. Figure 3 shows that the profiles of the wild type gave three peaks corresponding to 2,3,4-tri-*O*-Me-Rha, 3,4-di-*O*-Me-Rha, and 6-d-Tal (Fig. 3A), whereas Δgtf1 lacked 6-d-Tal (Fig. 3B) and Δgtf2 lacked 3,4-di-*O*-Me-Rha and 2,3,4-tri-*O*-Me-Rha (Fig. 3C). Complementation of both disruptants with each respective gene restored the TLC profile of GPLs to that observed for the wild type (not shown). Therefore, the *gtf1* and *gtf2* genes are found to be responsible for transferring the 6-d-Tal and Rha residues, respectively.

Structural determination of GPL-5 and GPL-6 for characterization of Δgtf3. The TLC profile of Δgtf3 showed that two spots (GPL-5 and GPL-6) disappeared (Fig. 2). To reveal the biosynthetic role of the *gtf3* gene, GPL-5 and GPL-6 were purified from mc^2155 and their structures were determined. GC/MS analyses showed that GPL-5 and GPL-6 contained 6-d-Tal and 3,4-di-*O*-Me-Rha, which were identified as sugar

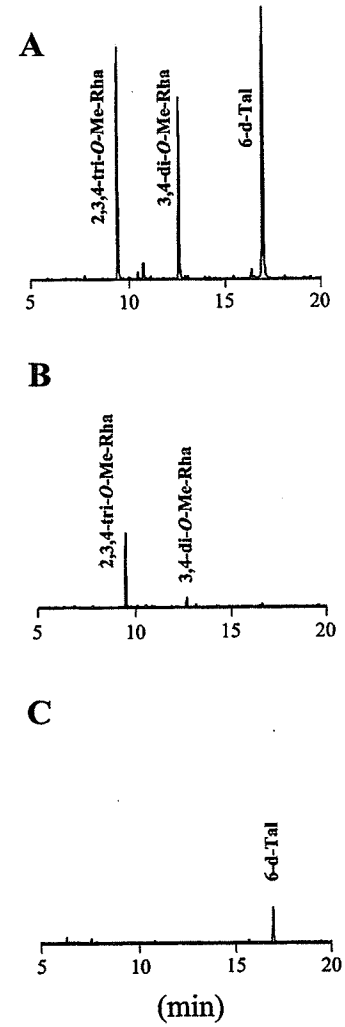

FIG. 3. GC/MS analyses of alditol acetates of sugars released from crude GPLs. GPLs were extracted from *M. smegmatis* strains: (A) mc^2155 strain, (B) Δgtf1, and (C) Δgtf2. Alditol acetate derivatives were prepared from the total lipid fraction after mild alkaline hydrolysis, which was extracted from an equal weight of harvested cells.

moieties of GPL-3 and GPL-4 (Fig. 4A). However, an extra sugar, 3-*O*-Me-Rha, was also detected (Fig. 4A). MALDI-TOF/MS analyses revealed that the main molecular ions of GPL-5 (*m/z* 1,333.8) and GPL-6 (*m/z* 1,319.8) were 160 mass units higher than those of GPL-3 (*m/z* 1,173.9) and GPL-4 (*m/z* 1,159.9), respectively (Fig. 4B). These results confirmed the presence of 3-*O*-Me-Rha in GPL-5 and GPL-6 and also suggested that 3-*O*-Me-Rha was further added to GPL-3 and GPL-4. Although GPL-5 and GPL-6 contained same three sugars, the spectra showed that the main molecular ion of GPL-5 (*m/z* 1,333.8) was 14 mass units higher than that of GPL-6 (*m/z* 1,319.8) (Fig. 4Ba and 4Bb). These differences in total mass may be due to O methylation of fatty acid as observed in structures of GPL-1 and GPL-3, suggesting that fatty acid of GPL-5 was O methylated like GPL-1 and GPL-3 (16). To investigate the sugar linked to D-*allo*-Thr of the fatty acyl-tetrapeptide core, GPL-5 and GPL-6 were subjected to β-elimination treatment. The main ion peaks of treated GPL-5 and

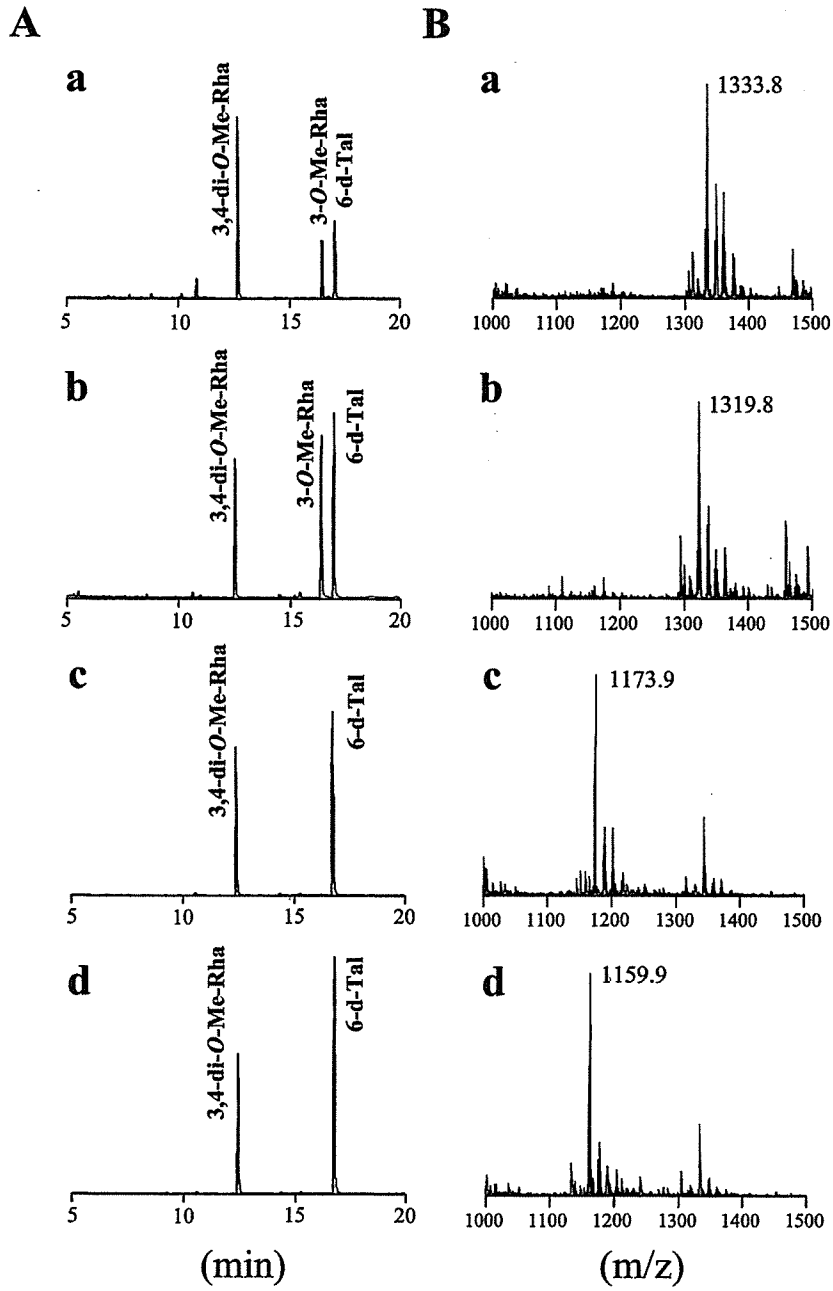

FIG. 4. Biochemical characterization of GPL-5 (a), GPL-6 (b), GPL-3 (c), and GPL-4 (d). (A) GC/MS analysis of alditol acetates of sugars released from each purified GPL. (B) MALDI-TOF/MS analysis of total molecular mass of each purified GPLs. (C) MALDI-TOF/MS analysis of total molecular mass of purified GPL-5 (a) and GPL-6 (b), which were subjected to β-elimination.

GPL-6 were *m/z* 1,171.7 and 1,157.7, respectively, which resulted in the loss of total mass of 162, suggesting that 6-d-Tal was linked to the position of D-*allo*-Thr (Fig. 4C). The linkage position of the sugars linked to the L-alaninol site of GPL-5 and GPL-6 was then determined by GC/MS analyses followed by perdeuteriomethylation. As shown in Fig. 5A, the GC profiles of alditol acetates from perdeuteriomethylated GPL-5 gave three peaks corresponding to 6-d-Tal, 3-*O*-Me-Rha, and 3,4-di-*O*-Me-Rha. The characteristic spectra of 3-*O*-Me-Rha and 3,4-di-*O*-Me-Rha, which are predicted to be linked to L-alaninol, are illustrated in Fig. 5B and C, respectively. The spectrum of 3-*O*-Me-Rha gave fragment ions at *m/z* 121, 134, and 165, which represent the presence of a deuteriomethyl group at positions C-2 and C-4. In contrast, no deuteriomethyl group was observed in 3,4-di-*O*-Me-Rha, whose C-2 position was acetylated, supported by the detection of fragment ions at *m/z* 131 and 190. The results from GC/MS analyses of perdeuteriomethylated GPL-6 were the same as those for GPL-5 (not shown). These observations demonstrated that GPL-5 and GPL-6 have the same sugar moieties, which are 6-d-Tal at

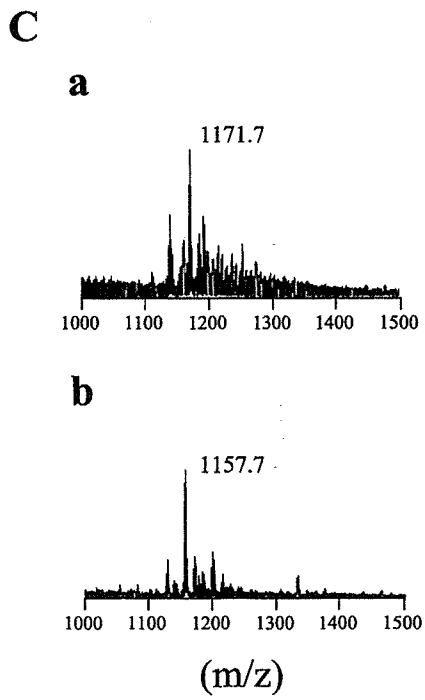

FIG. 4—*Continued.*

D-*allo*-Thr and 3-*O*-Me-rhamnosyl-(1→2)-3,4-di-*O*-Me-Rha at L-alaninol, indicating that 3-*O*-Me-Rha was linked to GPL-3 and GPL-4 (Fig. 6).

Overexpression of *gtf1*, *gtf2*, *gtf3*, and *gtf4* in *M. smegmatis* mc²155. To investigate the effects of overexpression of each gene on GPL biosynthesis, we constructed four *gtf*-overexpressed strains in wild-type mc²155 and compared the profile of total GPLs by TLC analyses. The results showed that the profiles of Wt/pMVgtf1, Wt/pMVgtf2, and Wt/pMVgtf4 were the same as that of Wt/pMV261, whereas Wt/pMVgtf3 produced two major compounds whose biochemical data corresponded to those of GPL-5 and GPL-6 (Fig. 7).

Characterization of *M. avium gtfA* and *gtfB*. We showed that both *M. smegmatis gtf1* and *gtf2* were responsible for glycosylation of the fatty acyl-tetrapeptide core. Comparison of the genome sequences encompassing the GPL biosynthetic gene cluster among several species of *M. avium* have shown that *gtfA* and *gtfB* (GenBank accession no. AF125999.1) are very similar to *M. smegmatis gtf1* and *gtf2*, respectively, in the corresponding putative amino acid sequences and might contribute to the glycosylation of the fatty acyl-tetrapeptide core (13). However, the function of each gene has not been thoroughly analyzed (13). Therefore, to confirm the role of *gtfA* and *gtfB*, we complemented Δgtf1 and Δgtf2 with the *gtf* expression vectors carrying *gtfA* (pMVgtfA) and *gtfB* (pMVgtfB). As shown in Fig. 8, TLC analyses revealed that *gtfA* and *gtfB* restored the production of wild-type GPLs in Δgtf1 and Δgtf2, respectively, whereas transformants with reverse vectors (Δgtf1/pMVgtfB and Δgtf2/pMVgtfA) did not produce wild-type GPLs. These results suggested that the function of *M. avium gtfA* and *gtfB* is the same as that of *M. smegmatis gtf1* and *gtf2*, respectively.

DISCUSSION

It has been shown that the *rtfA* gene of *M. avium* encodes a rhamnosyltransferase which synthesizes ssGPLs, while other genes involved in the glycosylation of the fatty acyl-tetrapeptide core remain unknown (12). In this study, we focused on the four genes of *M. smegmatis*, which show high similarity to *rtfA*, and generated their disruptants to characterize the role in the GPL biosynthesis.

In the early glycosylation steps of the fatty acyl-tetrapeptide core, we observed that the disruption of *gtf1* abolished the whole GPLs and led to the accumulation of *O*-Me-Rha derivatives without 6-d-Tal in Δgtf1 (Fig. 3B). Thus, we propose that the *gtf1* gene product catalyzes the transfer of 6-d-Tal to fatty acyl-tetrapeptide core. It is reported that the *M. avium* 104Rg strain, which has a spontaneous deletion in the genome region including *gtfA*, also accumulated *O*-methylated and nonmethylated Rha without 6-d-Tal (13, 30). This property is directly supported by our result that the *gtfA* could complement Δgtf1 (Fig. 8). However, *M. avium* 104Rg mainly contained nonmethylated Rha, whereas Δgtf1 derived from *M. smegmatis* mc²155 contained only *O*-Me-Rha. These different observations may be due to differences in the substrate specificity of methyltransferase, because 2,3,4-tri-*O*-Me-Rha was present in *M. smegmatis* mc²155 but was not identified in *M. avium* species (8, 25).

When the *gtf2* gene was disrupted, we detected 6-d-Tal without Rha derivatives in GC/MS analysis, which demonstrates that the *gtf2* gene contributes to the transfer of Rha to the fatty acyl-tetrapeptide core (Fig. 3C). In addition, complementation revealed that the *gtfB* gene of *M. avium* had the same function as *gtf2* (Fig. 8). In the previous studies of GPL biosyntheses, the mutant accumulating 6-d-Tal-containing derivatives without the Rha residue have not been isolated from GPL-producing species so far. Our results directly indicated for the first time that 6-d-Tal-containing derivatives could be an intermediate for the biosynthetic pathways of GPLs.

As for the order of glycosylation steps regulated by *gtf1* and *gtf2*, we cannot determine which step takes place earlier, since both disruptants accumulated the intermediates having different component (Fig. 3B and C). For *M. avium* serovar 2, Eckstein et al. proposed a pathway in which the transfer of the Rha residue to the fatty acyl-tetrapeptide core occurred prior to that of 6-d-Tal, because a mutant strain, 104Rg, having the *gtfA* region deleted, accumulated the fatty acyl-tetrapeptide core with only the Rha residue (13). However, our results lead to the interesting possibility that there are two alternative glycosylation pathways for the formation of nsGPLs (Fig. 9). If the glycosylation should occur in a single pathway, we would expect the accumulation of a nonglycosylated intermediate in either of the disruptants, because one of the genes, *gtf1* or *gtf2*, would be responsible for the first step of glycosylation converting the fatty acyl-tetrapeptide core to a glycosylated intermediate. Thus, the detection of glycosylated intermediates from both Δgtf1 and Δgtf2 suggests that (i) the fatty acyl-tetrapeptide core could be the substrate for both Gtf1 and Gtf2 and (ii) the glycosylated intermediates could also be the substrates for both Gtf1 and Gtf2. We prove here that Gtf1 and Gtf2 have broad substrate specificity and propose that the fatty acyl-tetrapeptide core is glycosylated by Gtf1 and Gtf2 at the same

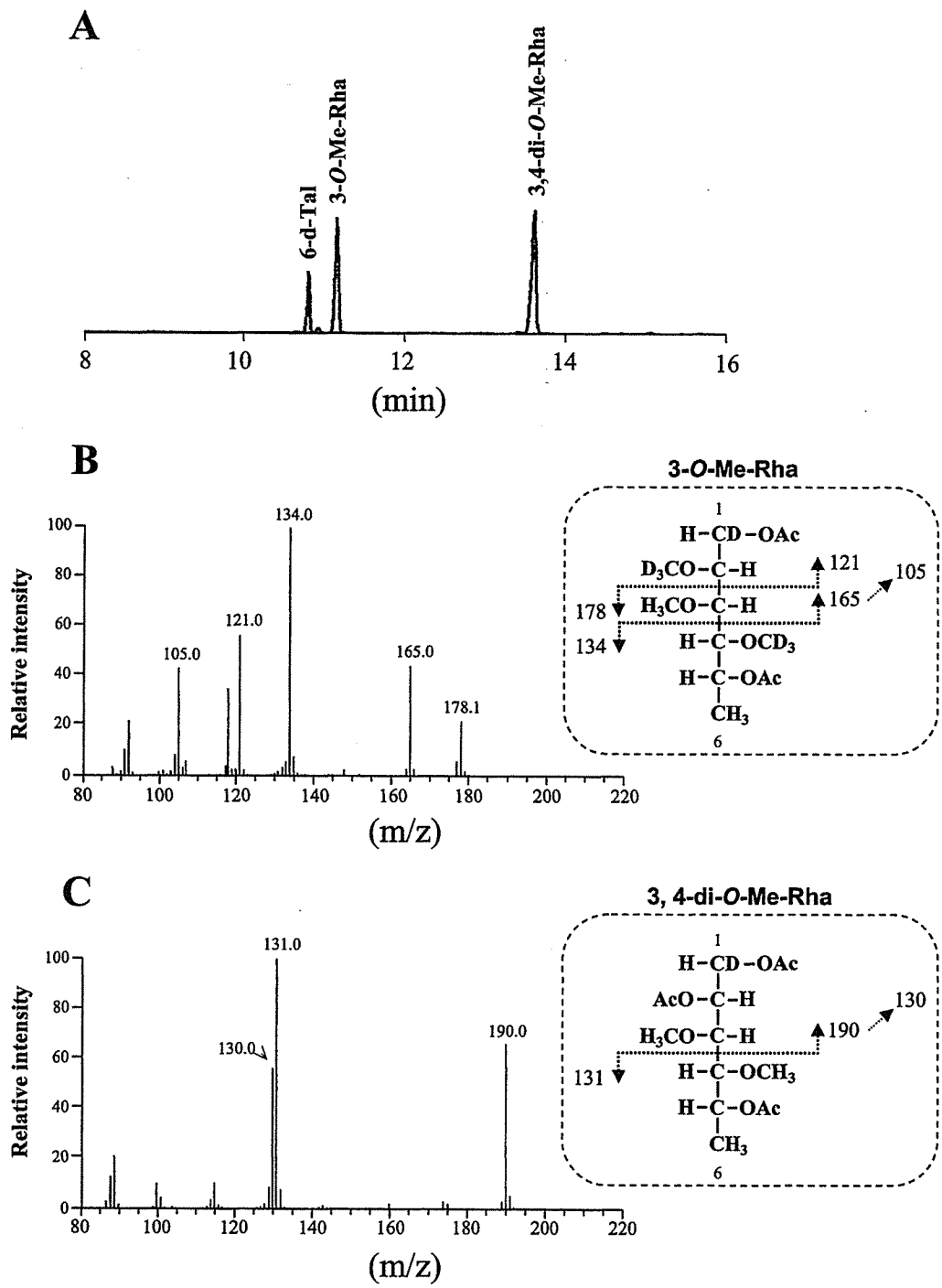

FIG. 5. GC/MS analysis of alditol acetates of sugars released from perdeuteriomethylated GPL-5. (A) GC profile. (B) Mass spectrum and fragment ion assignment corresponding to 3-*O*-Me-Rha. (C) Mass spectrum of fragment ion assignment corresponding to 3,4-di-*O*-Me-Rha.

time and then converted to the nsGPLs having both 6-d-Tal and *O*-Me-Rha via cross-glycosylations (Fig. 9).

Structural determination of GPL-5 and GPL-6 revealed that L-alaninol of the fatty acyl-tetrapeptide core was glycosylated with disaccharide (3-*O*-Me- and 3,4-di-*O*-Me-Rha), which was structurally different from GPLs including GPL-1 to -4 and ssGPLs (Fig. 6). However, it is reported that *M. fortuitum* complex produced GPLs which are glycosylated as in GPL-5 and GPL-6 as major components (19, 20). Therefore, these observations suggest that this type of glycosylation is not specific for *M. smegmatis*. GC/MS analyses of GPL-5 and GPL-6 indicated the presence of 3-*O*-Me-Rha in addition to 3,4-di-*O*-Me-Rha, and analyses of perdeuteriomethylated GPL-5 and GPL-6 showed that position C-1 of 3-*O*-Me-Rha is linked to position C-2 of 3,4-di-*O*-Me-Rha. Recent studies have shown that *M. smegmatis* mc^2155 newly produces two polar GPLs

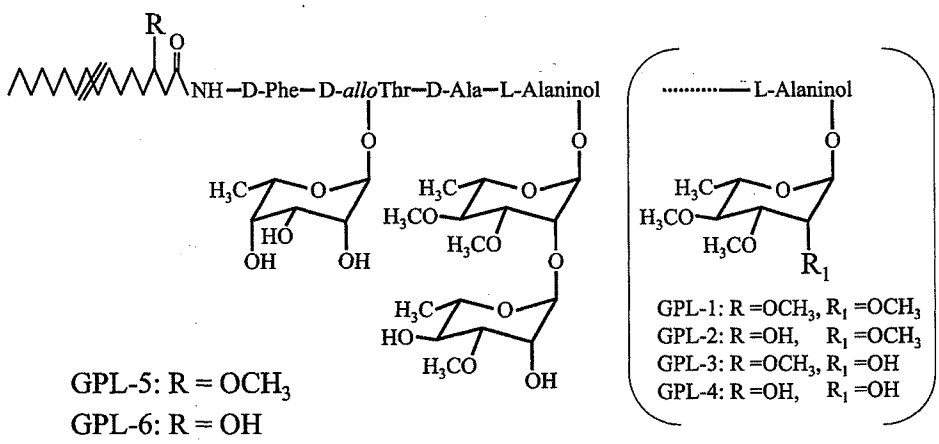

FIG. 6. Proposed structures of GPL-5 and GPL-6. Figure in parentheses shows the structure of GPL-1, GPL-2, GPL-3, and GPL-4, which were characterized in previous studies (10, 16, 25).

which contained two units of 3,4-di-*O*-Me-Rha at L-alaninol of the fatty acyl-tetrapeptide core with no 3-*O*-Me-Rha at any other position when cultured in carbon-limited medium (23, 24). However, the reason for not being able to detect 3-*O*-Me-Rha remains unknown.

In the *gtf3*-overexpressed strain Wt/pMVgtf3, the productivities of GPL-5 and GPL-6 were much higher than those of other GPLs (Fig. 7). So, we can speculate that the expression level of *gtf3* is usually repressed and could be regulated by some environmental factors, such as the nutrient condition or the gene encoding sigma factor (23, 24). GC/MS analyses showed that GPL-5 and GPL-6 have the structures in which 3-*O*-Me-Rha is linked to GPL-3 and GPL-4. These results suggest that GPL-3 and GPL-4 could be the precursors of GPL-5 and GPL-6, respectively, and in Wt/pMVgtf3, overexpression of *gtf3* resulted in 2-*O*-rhamnosylation of 3,4-di-*O*-Me-Rha in GPL-3 and GPL-4 instead of 2-*O*-methylation for converting to GPL-1 and GPL-2, so that GPL-5 and GPL-6 were synthesized.

Figure 9 represents proposed glycosylation steps related to *M. smegmatis* and *M. avium*. We showed that the functions of *gtf1* and *gtf2* corresponded to those of *gtfA* and *gtfB*, respectively. This finding demonstrates that the biosynthetic pathway for nsGPLs, which is the glycosylation of the fatty acyl-tetrapeptide core with the 6-d-Tal and Rha residues, is common between *M. smegmatis* and *M. avium*. Moreover, the biochemical characterization of Δgtf2 and Δgtf1 suggested that the glycosylation pathways for nsGPLs might not be stringent. On the other hand, it has been shown that the *rtfA* gene of *M. avium* triggers the biosynthesis of ssGPLs by transfer of Rha to 6-d-Tal of nsGPLs (12). In *M. smegmatis*, our results indicated that the *gtf3* gene plays a role in synthesis of 3-*O*-Me-rhamno-

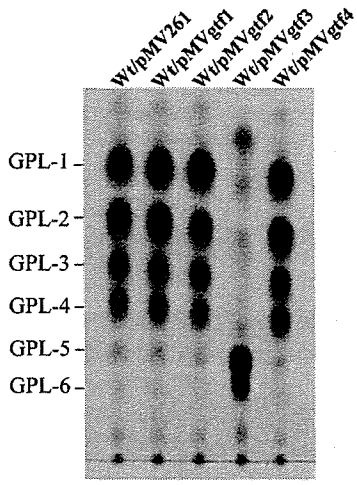

FIG. 7. TLC analyses of crude GPL extracts from the *M. smegmatis* mc^{2}155 strain (Wt) transformed with *gtf* expression vectors. Total lipid fraction after mild alkaline hydrolysis was spotted on plates and developed in $CHCl_3$-CH_3OH (9:1 [vol/vol]). GPLs were visualized by spraying with 10% H_2SO_4 and charring. Each total lipid fraction was extracted from an equal weight of harvested cells.

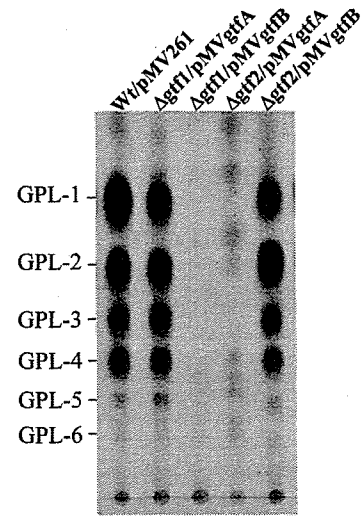

FIG. 8. TLC analyses of crude GPL extracts from the *M. smegmatis* mc^{2}155 strain (Wt) and its gene disruptants transformed with *M. avium* *gtfA* and *gtfB*. Total lipid fraction after mild alkaline hydrolysis was spotted on plates and developed in $CHCl_3$-CH_3OH (9:1 [vol/vol]). GPLs were visualized by spraying with 10% H_2SO_4 and charring. Each total lipid fraction was extracted from an equal weight of harvested cells.

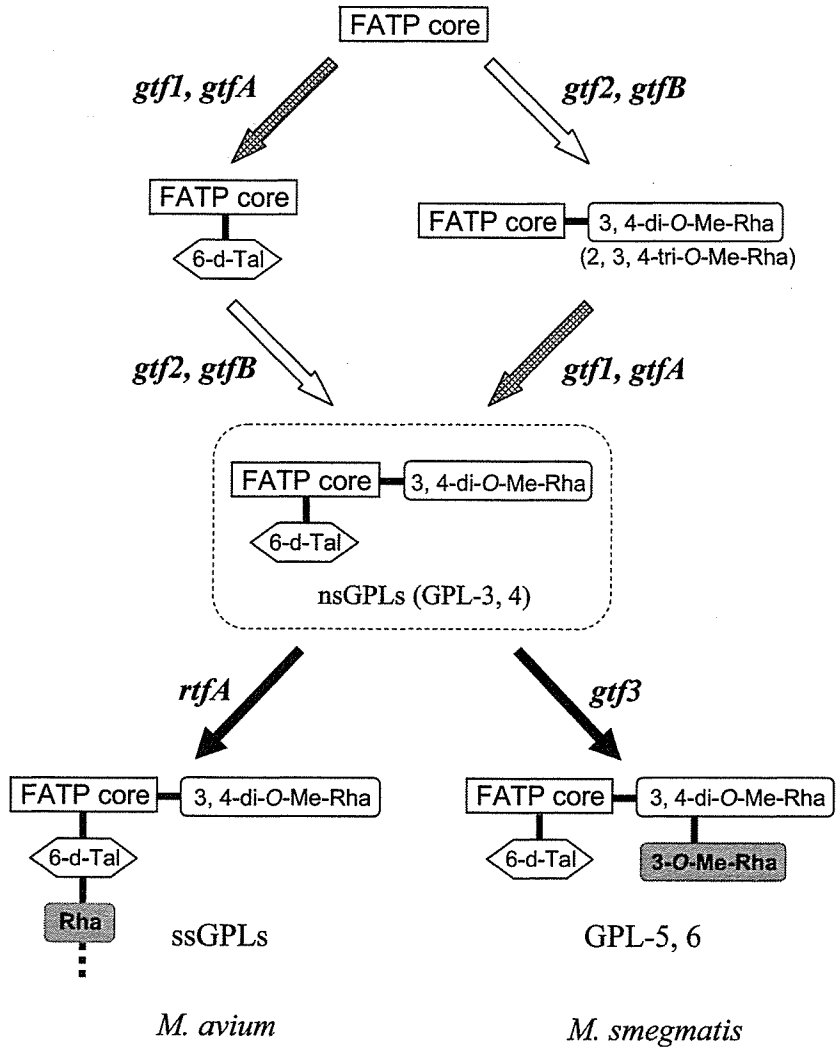

FIG. 9. Proposed biosynthetic pathways for GPLs of *M. smegmatis* and *M. avium*. FATP core, fatty acyl-tetrapeptide core.

syl-(1→2)-3,4-di-*O*-Me-Rha linked to L-alaninol of the fatty acyl-tetrapeptide core by transfer of an extra Rha residue to nsGPLs. Thus, the *rtfA* and *gtf3* genes have the ability to confer the biosynthetic differences between *M. avium* and *M. smegmatis*, suggesting that these genes may be responsible for the phylogenetic distinctions in the two species of mycobacteria.

ACKNOWLEDGMENTS

We thank W. R. Jacobs, Jr. (Albert Einstein College of Medicine, N.Y.), for providing us with the specialized transducing phage system.

This work was supported in part by grants from Health Science Research Grants—Research on Emerging and Re-emerging Infectious Diseases, Grant-in-Aid for Research on HIV/AIDS, the Ministry of Health, Labor and Welfare, Japan.

REFERENCES

1. **Aspinall, G. O., D. Chatterjee, and P. J. Brennan.** 1995. The variable surface glycolipids of mycobacteria: structures, synthesis of epitopes, and biological properties. Adv. Carbohydr. Chem. Biochem. **51:**169–242.
2. **Bardarov, S., S. Bardarov, Jr., M. S. Pavelka, Jr., V. Sambandamurthy, M. Larsen, J. Tufariello, J. Chan, G. Hatfull, and W. R. Jacobs, Jr.** 2002. Specialized transduction: an efficient method for generating marked and unmarked targeted gene disruptions in *Mycobacterium tuberculosis*, *M. bovis* BCG, and *M. smegmatis*. Microbiology **148:**3007–3017.
3. **Barrow, W. W., T. L. Davis, E. L. Wright, V. Labrousse, M. Bachelet, and N. Rastogi.** 1995. Immunomodulatory spectrum of lipids associated with *Mycobacterium avium* serovar 8. Infect. Immun. **63:**126–133.
4. **Belisle, J. T., K. Klaczkiewicz, P. J. Brennan, W. R. Jacobs, Jr., and J. M. Inamine.** 1993. Rough morphological variants of *Mycobacterium avium*. Characterization of genomic deletions resulting in the loss of glycopeptidolipid expression. J. Biol. Chem. **268:**10517–10523.
5. **Billman-Jacobe, H., M. J. McConville, R. E. Haites, S. Kovacevic, and R. L. Coppel.** 1999. Identification of a peptide synthetase involved in the biosynthesis of glycopeptidolipids of *Mycobacterium smegmatis*. Mol. Microbiol. **33:**1244–1253.
6. **Bjorndal, H., C. G. Hellerqvist, B. Lindberg, and S. Svensson.** 1970. Gas-liquid chromatography and mass spectrometry in methylation analysis of polysaccharides. Angew. Chem. Int. Ed. **9:**610–619.
7. **Brennan, P. J., and H. Nikaido.** 1995. The envelope of mycobacteria. Annu. Rev. Biochem. **64:**29–63.
8. **Chatterjee, D., and K. H. Khoo.** 2001. The surface glycopeptidolipids of mycobacteria: structures and biological properties. Cell. Mol. Life Sci. **58:** 2018–2042.
9. **Ciucanu, I., and F. Kerek.** 1984. A simple and rapid method for the permethylation of carbohydrates. Carbohydr. Res. **131:**209–217.
10. **Daffe, M., M. A. Laneelle, and G. Puzo.** 1983. Structural elucidation by field desorption and electron-impact mass spectrometry of the C-mycosides isolated from *Mycobacterium smegmatis*. Biochim. Biophys. Acta **751:**439–443.
11. **Daffe, M., and P. Draper.** 1998. The envelope layers of mycobacteria with reference to their pathogenicity. Adv. Microb. Physiol. **39:**131–203.
12. **Eckstein, T. M., F. S. Silbaq, D. Chatterjee, N. J. Kelly, P. J. Brennan, and J. T. Belisle.** 1998. Identification and recombinant expression of a *Mycobac-*